GEOPHYSICAL RESEARCH LETTERS, VOL. 27, NO. 17, PAGES 2605-2608, SEPTEMBER 1, 2000

Ozone destruction and production rates between spring and autumn in the Arctic stratosphere

D. W. Fahey[1,2], R. S. Gao[1,2], L. A. Del Negro[3], E. R. Keim[4], S. R. Kawa[5], R. J. Salawitch[6], P. O. Wennberg[7], T. F. Hanisco[8], E. J. Lanzendorf[8], K. K. Perkins[8], S. A. Lloyd[9], W. H. Swartz[9,10], M. H. Proffitt[1,2], J. J. Margitan[6], J. C. Wilson[11], R. M. Stimpfle[8], R. C. Cohen[12], C. T. McElroy[13], C. R. Webster[6], M. Loewenstein[14], J. W. Elkins[3], T. P. Bui[14]

Abstract. In situ measurements of radical and long-lived species were made in the lower Arctic stratosphere (18 to 20 km) between spring and early autumn in 1997. The measurements include O_3, ClO, OH, HO_2, NO, NO_2, N_2O, CO, and overhead O_3. A photochemical box model constrained by these and other observations is used to compute the diurnally averaged destruction and production rates of O_3 in this region. The rates show a strong dependence on solar exposure and ambient O_3. Total destruction rates, which reach 19%/month in summer, reveal the predominant role of NO_x and HO_x catalytic cycles throughout the period. Production of O_3 is significant only in midsummer air parcels. A comparison of observed O_3 changes with destruction rates and transport effects indicates the predominant role of destruction in spring and an increased role of transport by early autumn.

Introduction

Measurements of a wide range of reactive and long-lived species were obtained in the lower stratosphere using the NASA ER-2 high-altitude research aircraft as part of the Photochemistry of Ozone Loss in the Arctic Region In Summer (POLARIS) project in 1997. POLARIS was designed to explore the decrease of O_3 that occurs between spring and autumn at northern high latitudes [*Newman et al.*, 1999; *Fahey and Ravishankara,* 1999]. Ozone destruction and production rates in sampled air masses are calculated using a photochemical box model constrained by the available in situ and remote observations.

[1]Aeronomy Laboratory, National Oceanic and Atmospheric Administration, Boulder, CO
[2]Cooperative Institute for Research in Environmental Sciences, University of Colorado, Boulder, CO
[3]NOAA Climate Monitoring and Diagnostics Laboratory, Boulder, CO
[4]The Aerospace Corporation, Los Angeles, CA
[5]NASA Goddard Space Flight Center, Greenbelt, MD
[6]NASA Jet Propulsion Laboratory, Pasadena, CA
[7]Division of Geology and Planetary Sciences, California Institute of Technology, Pasadena, CA
[8]Department of Chemistry, Harvard University, Cambridge, MA
[9]The Johns Hopkins University Applied Physics Laboratory, Laurel, MD
[10]Department of Chemistry and Biochemistry, University of Maryland, College Park, MD
[11]Department of Engineering, University of Denver, Denver, CO
[12]Department of Chemistry, University of California, Berkeley, CA
[13]Atmospheric Environment Service, Downsview, Ontario, Canada
[14]NASA Ames Research Center, Moffett Field, CA

Paper number 2000GL011404.
0094-8276/00/2000GL011404$05.00

O_3 destruction and production processes

Stratospheric O_3 abundances represent a balance between destruction and production processes and transport. The reactions listed in Table 1 represent the principal chemical processes controlling O_3 production and destruction in the lower summer stratosphere [*Nevison et al.*, 1999; *Lary et al.*, 1997]. Ozone is destroyed in catalytic cycles involving nitrogen, hydrogen, chlorine, and bromine species and in reaction with O atoms. Ozone production occurs primarily through oxygen photolysis (R14). Production terms from CO and CH_4 oxidation are small and are neglected here. The destruction and production terms associated with the processes in Table 1 are grouped in Table 2. The grouping by reactive family is not unique since some catalytic cycles involve reactive species from more than one family. The terms use [X] for the concentration of species X, k_i for the kinetic rate coefficient of R_i, j_i for the photolysis rate coefficient of R_i, and C_i for branching terms. The O_3 destruction and production rates for an air parcel are obtained by integration of the terms in Table 2 over a diurnal cycle. In addition to rate coefficients and pressure, the integration requires the diurnal abundances of 12 species: OH, HO_2, NO, NO_2, ClO, BrO, $ClONO_2$, $BrONO_2$, O, O_2, O_3, and CO.

Observed and derived parameters

Measurements provided by instruments on board the ER-2 aircraft are used directly and indirectly to constrain a photochemical box model and the integration of diurnal O_3 change. Those used here are NO, NO_2, OH, ClO, CO, O_3, NO_y, N_2O, halon-1211, CFC-11, SF_6, surface area (SA) of background sulfate aerosol, overhead O_3 column, effective surface reflectivity, pressure (P), temperature (T), latitude, longitude, and measurement time. The source and uncertainty for most of these in situ measurements are described elsewhere [*Del Negro et al.*, 1999; *Gao et al.*, 1997; *Herman et al.*, 1999]. An air parcel is defined by a 100s average measurement along the flight track when the solar zenith angle (SZAs) is less than 85°. The full diurnal dependences of OH and ClO are estimated for each air parcel by scaling the SZA relationships in *Wennberg et al.* [1994] to the respective air parcel measurement.

Photolysis rate coefficients for an air parcel are available from two independent calculations [*Salawitch et al.*, 1994; *Swartz et al.*, 1999]. Both calculations use a spherical, isotropic multiple-scattering model of the atmospheric radiation field, incorporating photolysis cross-sections, observed overhead O_3 (column amount above the aircraft), and surface reflectivity. Changes in overhead O_3 vary from climatological values along the flight track, significantly affecting the local radiation field. The j values calculated for POLARIS generally show good agreement (±15%) with each other [*Del Negro et al.*, 1999]. Values of j_{15}, O_3, and pressure are combined to calculate the diurnal dependence of O atoms using the steady state relation $[O] = j_{15}[O_3]/k_{16}[O_2][M]$.

A diurnal photochemical box model is used here to calculate the diurnal dependence of NO_2, HO_2, $ClONO_2$, $BrONO_2$, and

Table 1. Reactions used in diurnal integration of O_3 change.

1	$OH+O_3 \rightarrow HO_2+2O_2$	10	$BrO+ClO \rightarrow Br+Cl+O_2$
2	$HO_2+O_3 \rightarrow OH+O_2$	11	$BrONO_2+h\nu \rightarrow Br+NO_3$
3	$ClO+HO_2 \rightarrow HOCl+O_2$	12	$NO_2+O(^3P) \rightarrow NO+O_2$
4	$BrO+HO_2 \rightarrow HOBr+O_2$	13	$O(^3P)+O_3 \rightarrow 2O_2$
5	$ClO+O(^3P) \rightarrow Cl+O_2$	14	$O_2+h\nu \rightarrow 2O(^3P)$
6	$ClONO_2+h\nu \rightarrow Cl+NO_3$	15	$O_3+h\nu \rightarrow O(^3P)+O_2$
7	$NO_3+h\nu \rightarrow NO+O_2$	16	$O(^3P)+O_2+M \rightarrow O_3+M$
8	$NO_3+h\nu \rightarrow NO_2+O$	17	$OH+CO+O_2 \rightarrow HO_2+CO_2$
9	$BrO+O(^3P) \rightarrow Br+O_2$	18	$HO_2+NO \rightarrow OH+NO_2$

BrO. The model includes the NO_y interconversion reactions as used by *Gao et al.* [1999] to simulate the NO_x/NO_y ratio in POLARIS. All rate coefficients are from *DeMore et al.* [1997] except for the OH + HNO_3, OH + NO_2 , and NO_2 + O reactions [see references in Portmann *et al.*, 1999]. Observed SA values (0.5 – 1.5 $\mu m^2 cm^{-3}$) are included in the model to determine the rate of the heterogeneous reactions N_2O_5 + H_2O and $BrONO_2$ + H_2O [*DeMore et al.*, 1997]. Other heterogeneous reactions are not important at POLARIS temperatures (~ 220 – 230 K) [*Del Negro et al.*, 1999]. Initial BrO concentrations for the box model are provided by calculations of the steady state partitioning of the Br_y reservoir. Br_y in an air parcel is estimated from the measurements of N_2O, halon-1211, CFC-11, and SF_6 as described in *Wamsley et al.* [1998]. The box model includes the principal inorganic bromine species and their interconversion reactions [*Lary et al.*, 1996].

The box model is constrained by measured ClO, the diurnal dependence of OH, and constant values of O_3, SA, Br_y, P, and T. The model is initialized with measured NO and NO_y and with approximate steady state values of NO_2, $ClONO_2$, N_2O_5, HNO_3, HO_2, and BrO. Good agreement has generally been found between measured and steady state values of NO_2, $ClONO_2$, and HO_2 in the lower stratosphere [*Del Negro et al.*, 1999; *Stimpfle et al.*, 1999; *Wennberg et al.*, 1994]. The model is integrated over 24 hrs from the measurement time using a 100s time step. After 24 hrs, output values of N_2O_5, $ClONO_2$, HNO_3, and BrO and the initial input values of NO and NO_y are used to reinitialize the model. Integration and reinitialization occurs for additional 24-hour periods (about 6) until further changes in N_2O_5, $ClONO_2$, HNO_3, and BrO values are negligible. With the model results and other parameters, O_3 destruction and production rates in an air parcel are obtained by integration of the respective processes in Table 2 over a diurnal cycle.

Results

The model and observational results are shown in Figure 1 for the spring, midsummer, and early autumn data as a function of latitude. Average total O_3 destruction rates at 18 to 20 km (panels A – C) are approximately 5%/month or greater throughout the data set with a maximum of about 19%/month above 80°N in midsummer. The total destruction rate is offset by O_3 production to yield the net destruction rate. The net O_3 destruction rates are positive (decreasing O_3 tendency) for all of POLARIS except for low latitudes in midsummer (panel B). The solar exposure (SE) values shown in panels D through F are the fraction of time that the SZA for an air parcel has been less than 93° in the past 1 or 5 days as calculated using back trajectories. SE values maximize in midsummer, reaching unity (continuous illumination) for parcels found poleward of 65°N. The difference between 1 and 5 day SE values is significant only for high latitudes in spring.

The fractional contributions to the total rates (panels D – F) by NO_x, HO_x, Cl/Br, and O processes indicates the predominant role of NO_x, particularly in the midsummer phase. The NO_x contribution correlates well with the average daytime NO_2 values (panels G – I) which range from 0.3 to 1.3 parts per billion by volume (ppbv). Since NO_y values are nearly constant (panels J – L), the NO_x/NO_y ratio changes in a similar manner to NO_2. The enhanced values of NO_2 and NO_x/NO_y in midsummer are attributed to the extent of continuous SE that occurs at high latitudes near solstice [*Farman et al.*, 1985; *Fahey and Ravishankara*, 1999; *Gao et al.*, 1999]. Continuous exposure of stratospheric air parcels causes N_2O_5 production to cease because NO_3, the intermediate in the production of N_2O_5, is rapidly photolyzed.

After NO_x, HO_x cycles are the next largest contributor (20 – 40%) to O_3 destruction rates in all phases. The smallest contributions are from the Cl/Br and O cycles which sum to about 20% in the spring and midsummer and slightly more in early autumn. The average mixing ratios of HO_2, ClO, and BrO are all less than 0.03 ppbv and significantly less than NO_2 values (panel G – I). The largest absolute values of the HO_2 and Cl/Br radicals and their largest contribution to O_3 destruction occur in early autumn. This is consistent with minimum values of NO_2 observed in late summer because NO_x moderates the abundance of these species [e.g. *Nevison et al.*, 1999; *Wennberg et al.*, 1994].

Forced increases in NO_x at constant NO_y do not proportionately increase modeled O_3 loss in the high-latitude summer stratosphere because of the NO_x moderating effect on the other loss cycles [*Nevison et al.*, 1999]. This was also confirmed with selected box model runs in the POLARIS data set. The POLARIS destruction rates depend more fundamentally on O_3 and SE as shown in Figure 2 for the data in Figure 1. The positive correlation of the rates with O_3 at constant SE is intriguing feature of the entire POLARIS data set. A similar correlation is also found separately in each phase. Underlying this correlation are the overall positive correlations of the daytime-averaged abundances of NO_2, HO_2, and ClO with O_3 in the data set (figures not shown). At constant O_3 in Figure 2, total destruction rates increase with SE. The SE changes are a combination of latitudinal and seasonal differences which are not separable here (Figure 1). Diurnally averaged destruction rates will in general depend strongly on SE since it increases with length-of-day and since destruction and production rates are zero at night. The extent to which the O_3 and SE dependences found here apply to other regions of the stratosphere must await further study.

The decrease in O_3 values in the POLARIS aircraft data set (60 - 70°N, 18-20 km) are very consistent (absolute values and month-to-month changes) with those in the more extensive satellite data sets [*Rosenlof*, 1999] and with the sonde/satellite climatology for 1988 to 1996 [*Logan and McPeters*; 1999]. Average O_3 values for 18 – 20 km for the month pairs April-May, June-July, and August-September are 2.6, 2.1, and 1.9 parts per million by volume (ppmv), respectively, from POLARIS and 2.4, 1.9, and 1.8 ppmv, respectively, from the climatology. The O_3 decreases in the aircraft data set are proportionately similar to

Table 2. O_3 destruction and production terms

Destruction	Term
by HO_x	$\{C_1 k_1[OH]+k_2[HO_2]\}[O_3]$
by NO_x	$2\,k_{12}[NO_2][O]$
by Cl/Br	$2\,(j_7/(j_7+j_8))\,\{j_6[ClONO_2]+j_{11}[BrONO_2]\}$ $(1+C_2)\{k_3[ClO]+k_4[BrO]\}[HO_2]$ $2\{k_5[ClO]+k_9[BrO]\}[O] + 2\,k_{10}[ClO]\,[BrO]$
by O	$2k_{13}[O][O_3]$
Production	**Term**
by O_2	$2\,j_{14}[O_2]$

Here $C_1 = k_2[O_3]/\{k_{18}[NO]+k_2[O_3]+k_3[ClO]+k_4[BrO]\}$
and $C_2 = k_1[O_3]/\{k_{17}[CO]+k_1[O_3]\}$

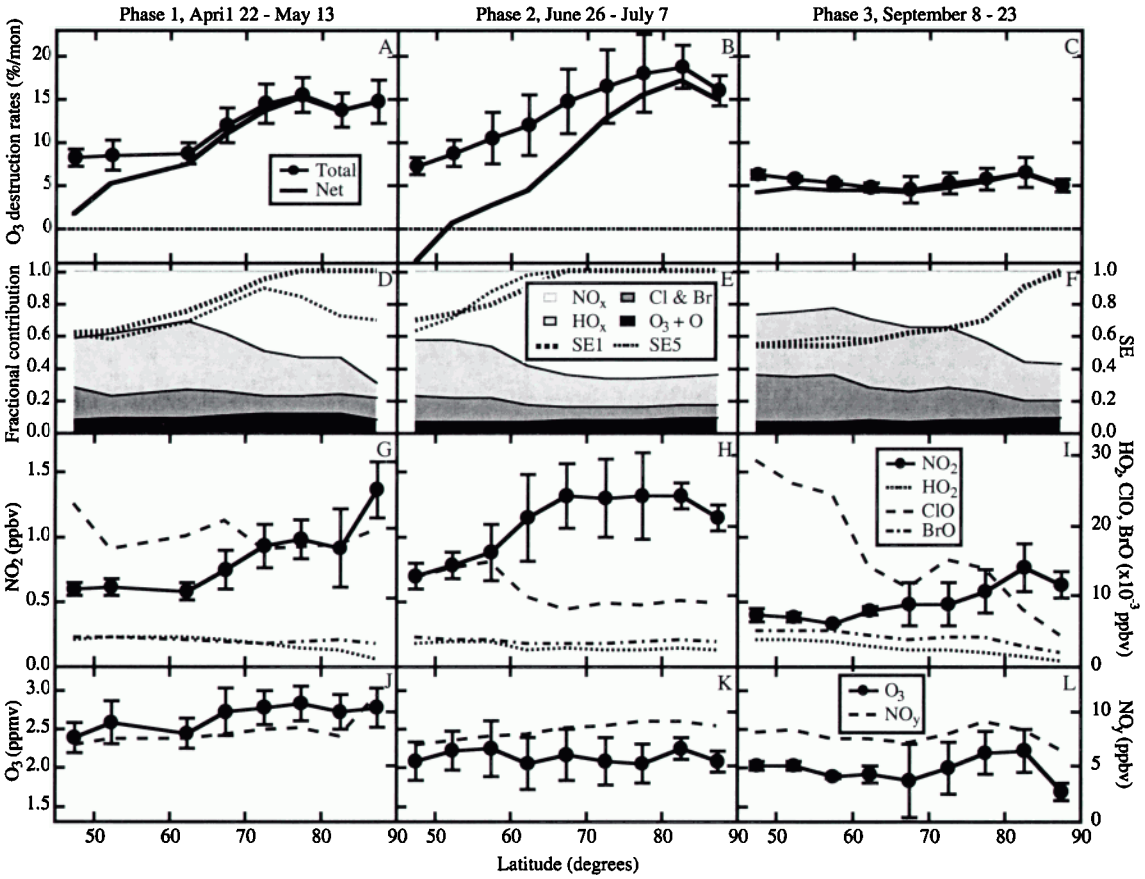

Figure 1. Observational data and results of the photochemical box model calculations as a function of northern latitude for the three phases of POLARIS. The total destruction rate is offset by the production rate to obtain the net destruction rate. Data are averages of sampled air parcels found in 5° latitude bins for ambient pressures between 50 and 80 hPa (~ 18 – 20 km). The number of flights and 100s data points included in each phase are, respectively, 9 and 600; 4 and 590; 6 and 530. More than one-half of the data points are obtained between 60°N and 70°N latitude in each phase. The lines in panels (D-F) are the calculated 1-day (thick-dashed) and 5-day (thin-dashed) solar exposure (SE) factors. Panels (D-F) represent the fractional contribution of the destruction processes in Table 2 to the total destruction rates. Panels (G-I) show the calculated daytime average mixing ratio of key radical species as used in the box model. Panels (J-L) show average observed O_3 and NO_y. The vertical bars show the sample variance in each latitude bin for the respective parameters. Ozone values are expressed as parts per million by volume (ppmv).

decreases in the associated O_3 column amounts [*Newman et al.*, 1999].

The net chemical destruction rates in Figure 1 for 60 – 70°N have been compared with observed O_3 changes and those inferred from modeled transport terms [*Rosenlof*, 1999]. In spring and midsummer the net destruction rates and observed rates of change (%/month) are very similar. In early autumn the net chemical destruction rate exceeds the observed rate of change. Transport processes are found to increase O_3 more strongly in early autumn than spring. A quantitative comparison indicates that spring and midsummer O_3 changes are dominated by chemical destruction whereas transport dominates in early autumn. Independent evidence for the predominant role of chemically induced O_3 changes in spring and summer comes from analysis of the O_3/HF column abundance ratios [*Toon et al.*, 1999] and fractal analysis of the O_3 data time series [*Tuck et al.*, 1999].

Summary and conclusions

In situ observations of radical and long-lived species made in the lower Arctic stratosphere (18 – 20 km) between spring and autumn of 1997 were combined with a photochemical box model to calculate total and net O_3 destruction rates. The rates are 10 – 20%/month in spring and midsummer, decreasing to near 5%/month in early autumn. Production of O_3 plays a significant role only in the Arctic summer period. The results show the predominance of the NO_x catalytic cycle over the HO_x and ClO/BrO cycles, arising from enhanced solar exposure. The

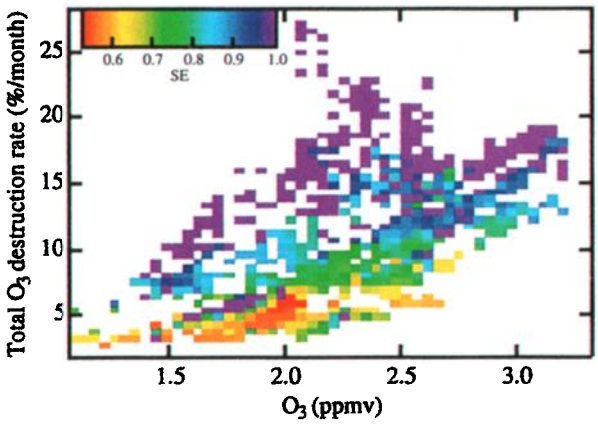

Figure 2. Total O_3 destruction rates from Figure 1 plotted versus observed O_3 in ppmv. The data points are 100s averages with the 1-day SE value indicated by the color legend.

destruction rates increase with solar exposure and ambient O_3 throughout the data set. A comparison with transport calculations show that chemical O_3 destruction predominates over transport effects in spring and that transport and chemical O_3 changes are more comparable in late summer/early autumn. Ozone destruction rates and transport processes are both altitude dependent. Hence, the results presented here may not be generalized to lower or higher altitudes. These results provide an observationally based reference point for the continued evaluation of observed spring/summer O_3 changes and of atmospheric models used to calculate present and future abundances of stratospheric O_3.

Acknowledgements The authors are grateful for support from the NASA Upper Atmospheric Research Program and the Atmospheric Effects of Aviation Project, to J. A. Logan for O_3 data, to P. A. Newman for backtrajectories, and to S. G. Donnelly for instrument support.

References

Del Negro, L. A., *et al.*, Comparison of modeled and observed values of NO_2 and J_{NO2} during the Photochemistry of Ozone Loss in the Arctic Region in Summer (POLARIS) mission, *J. Geophys. Res., 104*, 26687-26703, 1999.

DeMore, W. B., *et al.*, Chemical kinetics and photochemical data for use in stratospheric modeling, *JPL Publ. 97-4*, Jet Propul. Lab., Pasadena, Calif., 1997.

Fahey, D. W., and A. R. Ravishankara, Summer in the stratosphere, *Science, 285*, 208-210, 1999.

Farman, J. C., *et al.*, Ozone photochemistry in the Antarctic stratosphere in summer, *Q. J. R. Meteorol. Soc., 111*, 1013-1028, 1985.

Gao, R. S., *et al.*, Partitioning of the reactive nitrogen reservoir in the lower stratosphere of the southern hemisphere: Observations and modeling, *J. Geophys. Res., 102*, 3935-3949, 1997.

Gao, R. S., *et al.*, A comparison of observations and model simulations of NO_x/NO_y in the lower stratosphere, *Geophys. Res. Lett., 26*, 1153-1156, 1999.

Herman, R. L., *et al.*, Measurements of CO in the upper troposphere and lower stratosphere, *Chemosphere: Global Change Sci., 1*, 173-183, 1999.

Lary, D. J., Catalytic destruction of stratospheric ozone, *J. Geophys. Res., 102*, 21515-21526, 1997.

Lary, D. J., Gas phase atmospheric bromine photochemistry, *J. Geophys. Res., 101*, 1505-1516, 1996.

Logan, J. A., and R. D. McPeters, *Ozone climatology*, in Models and Measurements Intercomparison II, NASA/TM-1999-209554, 1999.

Newman, P. A., *et al.*, Preface to special section: Photochemistry of Ozone Loss in the Arctic Region in Summer (POLARIS), *J. Geophys. Res., 104*, 26481-26495, 1999.

Nevison, C. D., S. Solomon, and R. S. Gao, Buffering interactions in the modeled response of stratospheric O_3 to increased NO_x and HNO_3, *J. Geophys. Res., 104*, 3741-3754, 1999.

Portmann, R. W., *et al.*, Role of nitrogen oxides in the stratosphere: A reevaluation based on laboratory studies, *Geophys. Res. Lett., 26*, 2387-2390, 1999.

Rosenlof, K., Estimates of the seasonal cycle of mass and ozone transport at high northern latitudes, *J. Geophys. Res., 104*, 26511-26523, 1999.

Salawitch, R. S., *et al.*, The diurnal variation of hydrogen, nitrogen, and chlorine radicals: Implications for the heterogeneous production of HNO_2, *Geophys. Res. Lett., 21*, 2551-2554, 1994.

Stimpfle, R., *et al.*, The coupling of $ClONO_2$, ClO, and NO_2 in the lower stratosphere from in situ observations using the NASA ER-2 aircraft, *J. Geophys. Res., 104*, 26705-26714, 1999.

Swartz, W. H., *et al.*, A sensitivity study of photolysis rate coefficients during POLARIS, *J. Geophys. Res., 104*, 26725-26735, 1999.

Toon, G. C., *et al.*, Ground-based observations of Arctic O_3 loss during spring and summer 1997, *J. Geophys. Res., 104*, 26497-26510, 1999.

Tuck, A. F., S. J. Hovde, and M. H. Proffitt, Persistence in ozone scaling under the Hurst exponent as an indicator of the relative rates of chemistry and fluid mechanical mixing in the stratosphere, *J. Phys. Chem. A, 103*, 10445-10450, 1999.

Wamsley, P. R., *et al.*, Distribution of halon-1211 in the upper troposphere and lower stratosphere and the 1994 total bromine budget, *J. Geophys. Res., 103*, 1513-1526, 1998.

Wennberg, P. O., *et al.*, Removal of stratospheric O_3 by radicals: In situ measurements of OH, HO_2, NO, NO_2, ClO, and BrO, *Science, 266*, 398-404, 1994.

T. P. Bui and M. Loewenstein, NASA Ames Research Center, Moffett Field, CA 94035.

R. C. Cohen, Department of Chemistry, University of California, Berkeley, CA 94720.

L. A. Del Negro and J. W. Elkins, NOAA Climate Monitoring and Diagnostics Laboratory, Boulder, CO 80303.

D. W. Fahey, R. S. Gao, and M. H. Proffitt, NOAA Aeronomy Laboratory, Boulder, Colorado, and Cooperative Institute for Research in Environmental Sciences (CIRES), University of Colorado, Boulder, CO 80303. (MHP currently with WMO/AREP, Geneva Switzerland).

T. F. Hanisco, E. J. Lanzendorf, R. M. Stimpfle, K. K. Perkins, Department of Chemistry, Harvard University, Cambridge, MA 02138.

S. R. Kawa, NASA Goddard Space Flight Center, Greenbelt, MD 20771.

E. R. Keim, The Aerospace Corporation, Los Angeles, CA 90009.

S. A. Lloyd, The Johns Hopkins University Applied Physics Laboratory, Laurel, MD 20723.

J. J. Margitan, R. J. Salawitch, C. R. Webster, NASA Jet Propulsion Laboratory, Pasadena, CA 91109.

C. T. McElroy, Atmospheric Environment Service, Downsview, Ontario, Canada.

W. H. Swartz, The Johns Hopkins University Applied Physics Laboratory, Laurel, MD and Department of Chemistry and Biochemistry, University of Maryland, College Park, MD 20723.

P. O. Wennberg, California Institute of Technology, Pasadena, CA 91125.

J. C. Wilson, Department of Engineering, University of Denver, Denver, CO 80208.

(Received January 17, 2000; revised May 26, 2000; accepted June 16, 2000)